

# Photobleaching through glass micropipettes: Sodium channels without lateral mobility in the sarcolemma of frog skeletal muscle

(patch electrodes/voltage clamp/focal recording)

W. STÜHMER\* AND W. ALMERS

Department of Physiology and Biophysics, SJ-40, University of Washington, Seattle, Washington 98195

Communicated by Charles H. Sawyer, October 16, 1981

**ABSTRACT** Sodium currents were recorded from frog skeletal muscle by using fire-polished micropipettes to electrically isolate and voltage clamp a small patch of sarcolemma. Sodium current amplitude served as an assay for the number of functional sodium channels in the patch. With the pipette as a light guide, these channels were irradiated with ultraviolet (UV) light directed through a quartz fiber into the back end of the pipette. The UV light emerging from the pipette tip caused localized destruction of the sodium channels in the patch, reducing sodium current 3- to 5-fold during a 30–90 s irradiation. If sodium channels could diffuse laterally in the membrane, current from the patch should recover with time as fresh channels enter from neighboring areas. No such recovery was observed during observation for 1 hr after irradiation. Our results set an upper limit of  $10^{-12}$  cm<sup>2</sup>/s for the diffusion coefficient—1/1000th that of rhodopsin, a membrane protein in the cell membrane of retinal rods. It is suggested that sodium channels are anchored in the sarcolemma.

Lateral diffusion of membrane proteins in cell membranes has been observed by several techniques and by many authors, mostly in embryonic cells (e.g., refs. 1 and 2) and in various cell lines maintained in tissue culture (e.g., refs. 3 and 4). Less is known about cells taken from adult animals (5–7) and there is only one report concerning lateral protein mobility in an intact, fully differentiated excitable cell—acetylcholine (AcCho) receptors at the nerve–muscle junction of vertebrate muscle were found to be practically immobile (8).

One may question whether this immobility is typical for membrane proteins in excitable cells because AcCho receptors are concentrated in aggregates beneath the innervating nerve terminal and, in rat myotubes, are mobile when they are diffusely distributed (3). Thus, it seemed useful to explore in an adult excitable cell the lateral mobility of a membrane protein that is thought to be distributed over the entire sarcolemma. An example is the sodium channel, which mediates the propagation of electric impulses along nerve axons and muscle cells by allowing, at the appropriate membrane potential, an influx of Na<sup>+</sup> measurable as electric current. The lateral mobility of this or other membrane potential-dependent ionic channels has not previously been explored, even though membrane proteins of this class play a central role in neurophysiology.

In this study we combine photobleaching with patch voltage-clamp recording to measure the lateral mobility of sodium channels in frog muscle sarcolemma. Like junctional AcCho receptors (8), sodium channels appear to be essentially immobile. A preliminary report of this work has appeared.†

## MATERIALS AND METHODS

**Patch Voltage Clamp.** Our method builds on techniques described previously (9, 10) and is illustrated in Fig. 1a. A fire-

The publication costs of this article were defrayed in part by page charge payment. This article must therefore be hereby marked "advertisement" in accordance with 18 U. S. C. §1734 solely to indicate this fact.

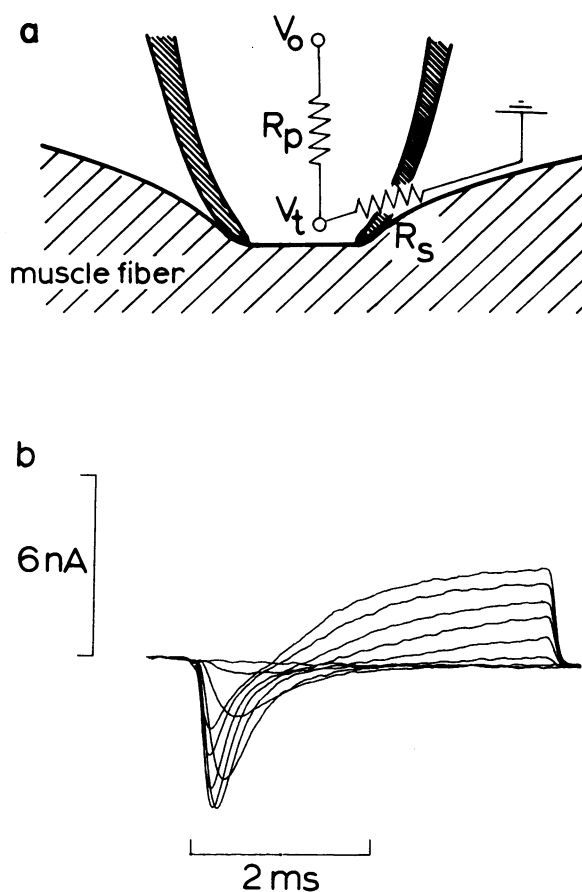


FIG. 1. (a) Schematic drawing of the system used to voltage clamp a patch of sarcolemma. (b) Membrane currents during nine depolarizing "test pulses" increasing in amplitude from 40 to 120 mV in increments of 10 mV. "Control pulses" for measuring the leakage current signal through  $R_s$  were half the amplitude of test pulses. They were superimposed on a 30-mV hyperpolarizing bias potential to prevent them from opening sodium channels. Test pulses were preceded by a 200-ms, 30-mV hyperpolarization to return to a functional state any channels that remained refractory at the fiber's resting potential. Fiber 1152; pipette tip diameter, 18  $\mu$ m;  $R_p = 0.54$  M $\Omega$ ; ( $R_s + R_p$ ) = 1.4 M $\Omega$ ; temperature, 17°C.

polished glass micropipette (see Fig. 2) is filled with Ringer's fluid (115 mM NaCl/1.8 mM CaCl<sub>2</sub>/2.5 mM KCl/3 mM morpholinopropanesulfonate buffer, pH 7.0) and presses against a

Abbreviations: UV, ultraviolet; AcCho, acetylcholine.

\* Present address: Fachbereich Physik, E-17, Technische Universität München, 8046 Garching b. München, Fed. Repub. of Germany.

† Stühmer, W. & Almers, W. (1981) Seventh International Biophysics Congress and Third Pan-American Biochemistry Congress, Mexico City, Mexico, August 1981, p. 179 (abstr.).

frog muscle fiber (*Rana temporaria*), electrically isolating a 10- $\mu\text{m}$ -diameter circular patch of sarcolemma beneath its tip. The membrane potential in the patch is displaced from the resting value (usually about  $-90$  mV, intracellular minus extracellular) by applying calibrated potential steps of amplitude  $V_o$  to the inside of the pipette. This is expected to result, at the pipette tip, in a potential change of amplitude  $V_t = AV_o$  where the attenuation factor  $A$  is given by

$$A = R_s / (R_p + R_s).$$

$R_p$  is the pipette resistance (typically 0.5–0.8 M $\Omega$ ) and  $R_s$  is the “seal” or “shunt” resistance to current flowing beneath the pipette rim (typically 0.9–2.5 M $\Omega$ ).  $R_p$  and  $(R_p + R_s)$  were measured as the resistances into the pipette before and after the pipette tip contacted the muscle fiber; we assumed the resting

conductance of the sarcolemmal patch to be negligible compared to  $1/(R_p + R_s)$ . During the experiment a digital computer measured  $(R_p + R_s)$  continually and applied potential steps of amplitude  $V_o$ , calculated to result in a potential change  $V_t$  of the desired amplitude. Measurements with intracellular microelectrodes showed that even with large (up to 15 nA) active currents across the patch, the internal potential changed by  $<1$  mV, so we assume that  $V_t$  is experienced by the sarcolemmal patch as a membrane potential change of equal size but opposite sign.

**Patch Current Recording.** Because we avoided enzymatic pretreatment of muscle fibers to remove collagen and the basal lamina,  $R_s$  here is less than in previous work (11) and most of the pipette current during a voltage step flows through  $R_s$ . However, with Ringer’s fluid inside and outside the pipette,  $R_s$  was highly linear and could be measured accurately by ap-

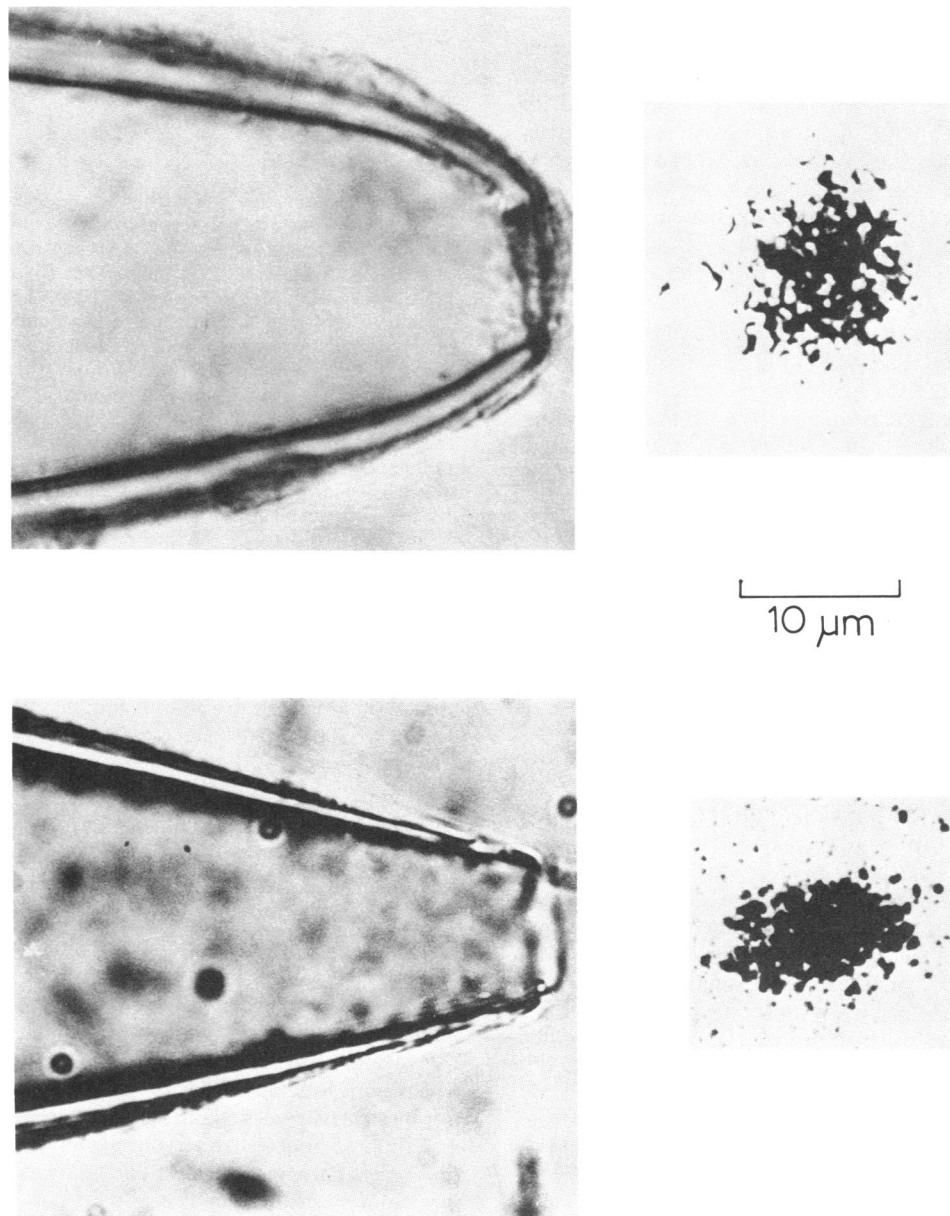


FIG. 2. (Left) Tips of two micropipettes used for voltage clamping and photobleaching of sodium channels. (Right) Images of the light beams emerging from the pipettes, made by pushing the pipette against photographic film (Kodalith Ortho 2556) and delivering highly attenuated 0.4- to 1-s flashes of 302-nm light through the pipettes. The developed film was then photographed through a  $\times 100$  oil immersion objective (n.a. 1.4). (Upper Left) This electrode had previously been used for the experiment in Figs. 3 and 4.

plying potential steps too small to open sodium channels. By using a combination of analog and digital techniques (12, 13), pipette currents during these steps could be scaled up appropriately and subtracted from currents during larger steps, so that only "active" currents through sodium channels remained after the subtraction. Currents were recorded through a 4-pole Bessel filter (5 kHz corner frequency) and sampled at 50 kHz by a 12-bit A/D converter. Measured currents were divided by the attenuation factor  $A$  to allow for loss of active current through  $R_s$  (11); the ordinate scales in our figures include this correction.

**Photobleaching.** Light from a high-pressure mercury arc lamp (Wotan 100-B) was directed through a mirror-and-filter system passing the 302-nm mercury line or a broader band including the 280- to 313-nm mercury lines. The light was focussed through a reflecting objective (Beck,  $\times 15$ , n.a. 0.28) onto a quartz fiber (Math Associates, Port Washington, NY) whose other end directed the light into the glass micropipette. With the pipette of Fig. 2 (Lower) the light emerging from the tip had a power of maximally 15 nW, as measured by passing the tip through a 200- $\mu\text{m}$ -diameter pinhole covering a UV-sensitive photodiode (HUV-4000B, EG&G, Salem, MA). If the light intensity at the pipette tip has a Gaussian profile decreasing by a factor of  $e^2$  (to 14%) within a radius of 5  $\mu\text{m}$ , then 15 nW would correspond to a peak intensity of  $\approx 38 \text{ mW/cm}^2$  (14). Irradiation with this pipette reduced sodium current about  $e$ -fold in 60 s.

## RESULTS

Fig. 1*b* shows membrane currents drawn from the pipette during depolarizing potential steps 40 to 120 mV in amplitude; the currents were corrected for leakage currents through  $R_s$  by analog circuitry and a digital computer. We believe that the inward (downwards) and outward (upwards) currents flow through voltage-sensitive sodium and potassium channels, respectively, because they show the kinetics and voltage dependence expected for currents through these channels (15, 16). Also, inward current is blocked by tetrodotoxin, a specific blocker of sodium channels (see Fig. 3). Sodium and potassium currents were found to vary from animal to animal, both in their absolute and relative sizes. With sodium currents, the range of variation was nearly 10-fold and many fibers had only small or no potassium currents. Even on the same fiber, sodium and potassium currents at different locations could vary up to 4-fold in size.<sup>§</sup> Here we selected fibers with large sodium and only small potassium currents.

Because the pipette will depolarize only the small membrane patch covered by its tip, we expect to collect active currents from this area only. Thus, glass micropipettes are suitable for localized recording of membrane currents. They can also be used as light guides for local membrane illumination (Fig. 2) by directing light through a quartz fiber into the back end of the pipette. To test the distribution of light coming out of the tip, we pushed the pipette against a piece of photographic film, much as we would ordinarily push it against a muscle fiber. After delivery of a UV flash through the pipette, the film was developed and the resulting "spot" photographed. Fig. 2 shows the tips of two pipettes and the spots made with them. Evidently light emerges as a fairly well-defined beam with a diameter roughly equal to that of the pipette tip.

UV light destroys sodium channels (17–20), probably in a direct, one-photon interaction. In Fig. 3 we used the pipette

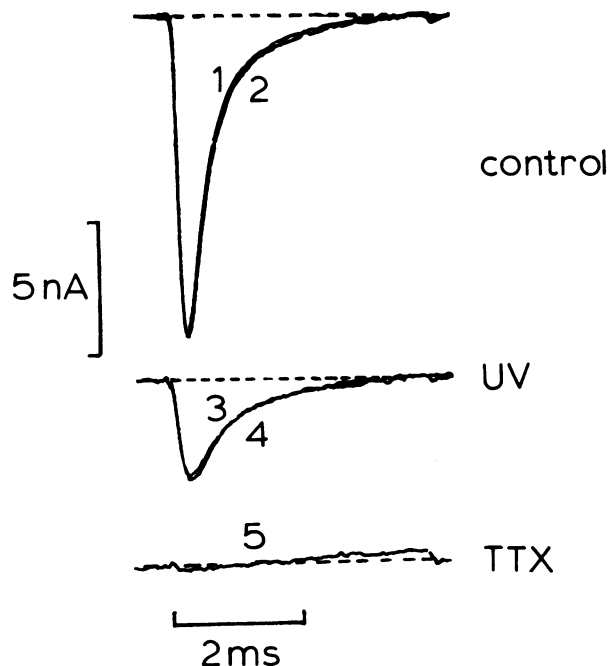


FIG. 3. Sodium currents during 80-mV depolarizations recorded before (Top; traces 1 and 2) and after (Middle; traces 3 and 4) UV irradiation. Each panel shows two traces superimposed; they were recorded with an interval of 30 min (Top) and 63 min (Middle). (Bottom) Trace 5 was recorded 2 min after applying  $\approx 1$  ml of 0.01 mM tetrodotoxin (TTX) to the bath which, if diluted uniformly, would yield a final concentration of 5–10  $\mu\text{M}$ . Fiber 1040;  $R_p = 0.65 \text{ M}\Omega$ ,  $R_s = 0.93 \text{ M}\Omega$ .  $R_s$  can be used to estimate the distance between pipette rim and sarcolemmal bilayer. Suppose the contact region between pipette rim and sarcolemma is filled with Ringer's fluid [resistivity, 89  $\Omega\text{cm}$  (21)], and shaped like a ring with inner and outer diameters of 10  $\mu\text{m}$  and 14  $\mu\text{m}$ , respectively. Then the radial resistance of the contact region would be equal to  $R_s$  if the vertical thickness of the space (i.e., the distance between pipette rim and sarcolemmal bilayer) is 100–200 nm. With a higher resistivity, the thickness of the space would be proportionately larger.

shown in Fig. 2 (Upper) to record from, and then to irradiate, a sarcolemmal patch. The figure shows pairs of superimposed current traces recorded during 80-mV step depolarizations. Traces 1 and 2 were recorded 0 and 30 min before, and traces 3 and 4 were recorded 1 and 63 min after a 90-s irradiation with UV. UV diminished the currents about 3-fold without strongly altering their time course. Lack of UV effects on kinetics, also observed by others (19, 20), indicates normal functioning of the surviving channels. Sixty minutes after irradiation, tetrodotoxin was added to the bath. Inward currents vanished (Fig. 3, trace 5) after a delay of 1–2 min, indicating that the toxin had reached the patch and that the surviving channels remained sensitive to it.

If fresh sodium channels from the neighboring, unirradiated membrane could reach the irradiated patch by lateral diffusion they would contribute to the recorded current, leading to recovery after irradiation. To test this point, peak sodium current during successive depolarizations is plotted against time in Fig. 4. Sodium current remained constant for 30 min, declined 3-fold during irradiation, and showed no recovery thereafter. Therefore, no new channels moved into the patch during our observation period. Three other experiments gave similar results. In a fourth,  $I_{Na}$  diminished about 6-fold during irradiation, remained constant for 20 min, and then regained half of its original amplitude within 5 min. We believe this unusual recovery to be an artifact and due to movement of the pipette relative to

<sup>§</sup> Almers, W., Stanfield, P. R. & Stühmer, W. (1981) Seventh International Biophysics Congress and Third Pan-American Biochemistry Congress, Mexico City, Mexico, August 1981, p. 303 (abstr.).

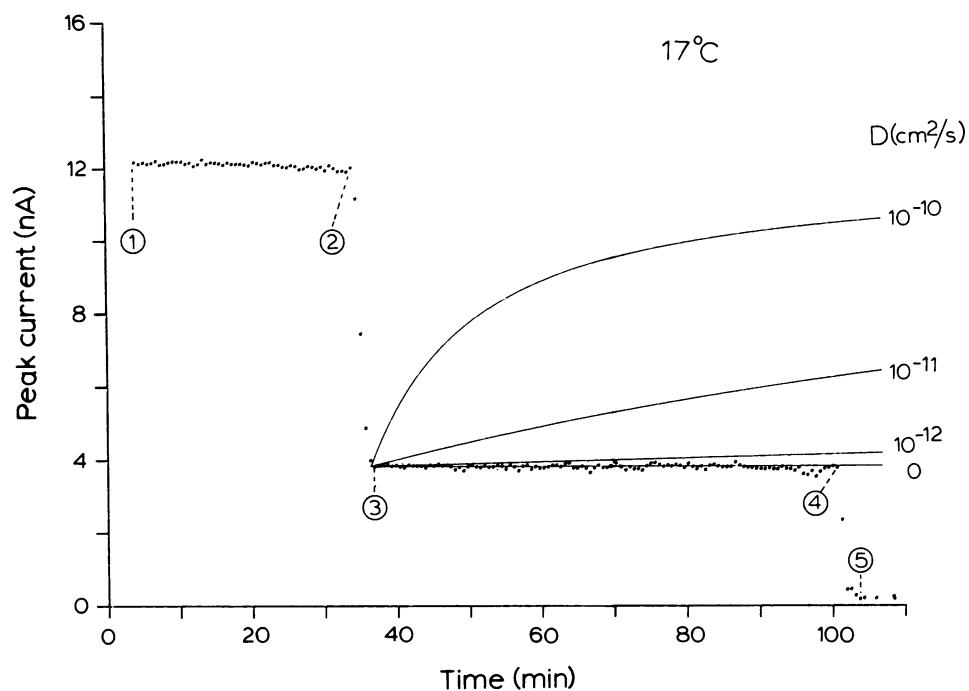


FIG. 4. Effect of UV light and tetrodotoxin on peak inward (sodium) currents during 80-mV step depolarizations. Same experiment as in Fig. 3; the circled numbers indicate the times at which the corresponding traces in Fig. 3 were recorded. The holding potential was displaced slightly (by 2–3 mV) in the depolarizing direction to keep the average potential at the pipette tip zero. This was done to prevent steady electric fields parallel to the membrane that might cause lateral redistribution of membrane constituents (4). Peak currents are given as absolute values and were measured by fitting a fourth-order polynomial to 0.6-ms sections of current traces starting 0.26 ms after the onset of depolarization and by taking the minimum of the fitted curve over that segment. Each point is the average of three measurements taken at 11.8-s intervals. Solid lines give  $I_p F(t)$ , in which  $I_p$  is the peak sodium current recorded before irradiation.  $F(t)$  is calculated by Eq. 1 with  $D$  as indicated,  $K = 2.999$ , and  $w = 5 \mu\text{m}$ ;  $t$  marks the time from the end of irradiation. In experiments of this kind, the slightest mechanical disturbance of muscle and pipette would bring sudden reappearance of sodium current. Attempts to “find” the irradiated spot again by probing the membrane area with the patch pipette were unsuccessful, consistent with our expectation from Fig. 2 that the photodestruction of sodium channels is highly localized. To avoid movement we worked on a vibration-isolation table floating on compressed air. After the pipette was placed onto the muscle fiber, the pipette holder was rigidly fixed to the experimental chamber by allowing a liquid wax linkage between holder and chamber to solidify.

the muscle fiber. Taken together, our results show that if lateral diffusion of sodium channels into the patch is possible, it must be very slow. They confirm a previous experiment with lower resolution (22) carried out with the “Vaseline gap” (16) technique.

In addition to lack of lateral mobility, one may consider two other reasons for the failure of channels to move into the irradiated patch. (i) Contact between pipette and sarcolemma mechanically restricts lateral motion. (ii) UV causes crosslinking of membrane or cytoskeletal components so the irradiated patch becomes a rigid structure into which fresh  $\text{Na}^+$  channels cannot penetrate. With regard to (i), we estimate the distance between pipette rim and the sarcolemmal bilayer to be about 100–200 nm (see Fig. 3 legend)—wider than the 20- to 30-nm-thick basal lamina covering the sarcolemma. To touch the pipette, integral membrane proteins would thus have to penetrate the basal lamina and extend beyond it for tens of nanometers, an unlikely possibility. Effects of fixed charges in the glass should also not extend far beyond 1 Debye length—about 1 nm in Ringer’s fluid. With regard to (ii), the energy deposited by our irradiation ( $\approx 2.5 \text{ J/cm}^2$ ) was only  $10^{-5}$  times that in photobleaching experiments with visible light in which lateral diffusion is observed (3). Also,  $\text{Na}^+$  and  $\text{K}^+$  channels surviving our irradiation appeared to operate normally. These considerations tend to argue against gross membrane alterations. However, possibility (ii) cannot be ruled out entirely and should be addressed in future experiments especially because any local immobilization of membrane proteins with partial retention of physiologic function could be a useful tool in cell physiology.

## DISCUSSION

To set an upper limit for the coefficient of lateral diffusion into the irradiated patch, we assumed that UV emerges from the pipette tip as a beam of Gaussian intensity profile, with the intensity decreasing by a factor of  $e^2$  within a distance  $w = 5 \mu\text{m}$  from the center of the orifice. We assume that the efficiency with which we record membrane current also varies laterally, being highest in the center of the patch and falling off in all directions along the same Gaussian curve. In reality both the beam profile and the area from which we record current are probably more sharply defined, so these are conservative assumptions. Recovery of current should then be given by

$$F(t) = \sum_{n=0}^{\infty} [(-K)^n/n!] [1 + n(1 + 2t/\tau_D)]^{-1}, \quad [1]$$

in which  $F(t)$  is the fractional current (peak current after irradiation/peak current before irradiation) and  $t$  is the time after irradiation (14). The parameter  $K$  is calculated from the fractional current immediately after irradiation,  $F(0)$ , by

$$F(0) = (1 - e^{-K})/K, \quad [2]$$

and  $\tau_D$  is related to the beam half-width,  $w$ , and the lateral diffusion coefficient,  $D$ , by

$$\tau_D = w^2/4D. \quad [3]$$

The curves in Fig. 4 show properly scaled solutions of Eq. 1 with  $D$  as indicated. A value of  $10^{-12} \text{ cm}^2/\text{s}$  appears to be the

limit of resolution in our experiment and may be taken as an upper limit for the lateral diffusion coefficient of sodium channels. This is much lower than values for rhodopsin in retinal rod cell membrane [ $4 \times 10^{-9} \text{ cm}^2/\text{s}$  (7)] or for extrajunctional AcCho receptors on rat myotubes [ $0.7 \times 10^{-10} \text{ cm}^2/\text{s}$  (3)] and on membrane "blebs" of mouse muscle [ $2 \times 10^{-9} \text{ cm}^2/\text{s}$  (8)], even though the molecular weights of AcCho receptors (23) and sodium channels (24) seem similar. If our result is representative for the unirradiated membrane, the comparison suggests that sodium channels are anchored in the sarcolemma of frog skeletal muscle. Their irregular lateral distribution and failure to electrophorese in response to large lateral electric fields may be taken as further evidence for this view.<sup>§</sup>

Lateral immobility of sodium channels may seem surprising. However, although sodium channels are not as discretely localized as AcCho receptors, they nevertheless populate the sarcolemma more densely than the membranes of the transverse tubular system (16, 22, 25). Lateral immobility may help maintain this uneven distribution over the cell membrane, which is important for reliable impulse propagation, both along and radially into the fiber (26). There is evidence for uneven distribution of membrane transport proteins also in other tissues. In rat myelinated nerve, sodium channels appear confined to the node of Ranvier (27)—a feature which aids in the well-known "saltatory" impulse propagation in that tissue. And in transporting epithelia, sodium pumps occur almost exclusively on the basolateral side of an epithelial cell (28, 29), thus insuring that transport is directional. In these and other examples, lack of lateral mobility could help in maintenance of the lateral segregation of some transport proteins throughout the life of the cell.

We thank Dr. C. E. Stirling for the use of his microscope and Drs. Bertil Hille, Peter B. Detwiler, and Peter R. Stanfield for reading the manuscript. This research was supported by grants from Muscular Dystrophy Association of America and National Institutes of Health Grant AM-17803. W.S. was supported by a fellowship from the Max Kade Foundation.

1. Edidin, M. & Wei, T. (1977) *J. Cell Biol.* **75**, 475–482.
2. Fishman, M. C., Dragsten, P. R. & Spector, I. (1980) *Nature (London)* **290**, 781–783.

3. Axelrod, D., Ravdin, P., Koppel, D. E., Schlessinger, J., Webb, W. W., Elson, E. L. & Podleski, T. R. (1976) *Proc. Natl. Acad. Sci. USA* **73**, 4594–4598.
4. Poo, M.-M., Poo, W.-J. H. & Lam, J. W. (1978) *J. Cell Biol.* **76**, 483–501.
5. Schindler, M., Koppel, D. E. & Scheetz, M. P. (1980) *Proc. Natl. Acad. Sci. USA* **77**, 1457–1461.
6. Dragsten, P. R., Henkart, P., Blumenthal, R., Weinstein, J. & Schlessinger, J. (1979) *Proc. Natl. Acad. Sci. USA* **76**, 5163–5167.
7. Wey, C.-L., Cone, R. A. & Edidin, M. A. (1981) *Biophys. J.* **33**, 225–232.
8. Tank, D. W., Wu, E. S. & Webb, W. W. (1981) *Biophys. J.* **33**, 74a (abstr.).
9. Strickholm, A. (1961) *J. Gen. Physiol.* **44**, 1073–1088.
10. Neher, E., Sakmann, B. & Steinbach, J. H. (1978) *Pflügers Arch.* **375**, 219–228.
11. Sigworth, F. & Neher, E. (1980) *Nature (London)* **286**, 71–73.
12. Bezanilla, F. & Armstrong, C. M. (1977) *J. Gen. Physiol.* **70**, 549–566.
13. Almers, W. & Palade, P. T. (1981) *J. Physiol. (London)* **312**, 159–176.
14. Axelrod, D., Koppel, D. E., Schlessinger, J., Elson, E. & Webb, W. W. (1976) *Biophys. J.* **16**, 1055–1069.
15. Adrian, R. H., Chandler, W. K. & Hodgkin, A. L. (1970) *J. Physiol. (London)* **208**, 607–644.
16. Hille, B. & Campbell, D. T. (1976) *J. Gen. Physiol.* **67**, 265–293.
17. Booth, J., von Muralt, A. & Stämpfli, R. (1950) *Helv. Physiol. Acta* **8**, 110–117.
18. Lüttgau, H.-C. (1956) *Pflügers Arch.* **262**, 244–255.
19. Fox, J. M. (1974) *Pflügers Arch.* **351**, 287–301.
20. Oxford, G. S. & Pooler, J. P. (1975) *J. Membr. Biol.* **20**, 13–26.
21. Adrian, R. H. & Almers, W. (1974) *J. Physiol. (London)* **237**, 573–605.
22. Almers, W., Fink, R. & Shepherd, N. in *Diseases of the Motor Unit*, ed. Schotland, D. L. (Wiley, New York), in press.
23. Raftery, M. A., Hunkapiller, M. W., Strader, C. D. & Hood, L. E. (1980) *Science* **208**, 1454–1457.
24. Hartshorne, R. P., Coppersmith, J. & Catterall, W. A. (1980) *J. Biol. Chem.* **255**, 10572–10575.
25. Jaimovitch, E., Venosa, R. A., Shrager, P. & Horowicz, P. (1976) *J. Gen. Physiol.* **67**, 399–416.
26. Adrian, R. H. & Peachey, L. D. (1973) *J. Physiol. (London)* **235**, 102–131.
27. Chiu, S. Y. & Ritchie, J. M. (1981) *J. Physiol. (London)* **313**, 415–438.
28. di Bona, D. R. & Mills, J. W. (1979) *Fed. Proc. Fed. Am. Soc. Exp. Biol.* **38**, 134–143.
29. Shaver, J. & Stirling, C. E. (1978) *J. Cell Biol.* **76**, 278–292.